Chemokine CCL20 promotes the paclitaxel resistance of $CD44^+CD117^+$ cells via the Notch1 signaling pathway in ovarian cancer

MIN CHEN[1,2*], JUAN SU[2*], CHUNMEI FENG[2], YING LIU[2], LI ZHAO[2] and YONGJIE TIAN[1]

[1]Department of Obstetrics and Gynecology, Shandong Provincial Hospital, Cheeloo College of Medicine, Shandong University, Jinan, Shandong 250021; [2]Department of Obstetrics and Gynecology, Taian City Central Hospital, Taian, Shandong 271000, P.R. China

Received December 15, 2020; Accepted May 11, 2021

DOI: 10.3892/mmr.2021.12274

Abstract. Studies have found that C-C motif chemokine ligand 20 (CCL20)/C-C motif chemokine receptor 6 (CCR6)/notch receptor 1 (Notch1) signaling serves an important role in various diseases, but its role and mechanism in ovarian cancer remains to be elucidated. The aim of the present study was to investigate the underlying mechanism of CCL20/CCR6/Notch1 signaling in paclitaxel (PTX) resistance of a $CD44^+CD117^+$ subgroup of cells in ovarian cancer. The $CD44^+CD117^+$ cells were isolated from SKOV3 cells, followed by determination of the PTX resistance and the CCR6/Notch1 axis. Notch1 was silenced in the $CD44^+CD117^+$ subgroup and these cells were treated with CCL20, followed by examination of PTX resistance and the CCR6/Notch1 axis. Furthermore, in nude mice, $CD44^+CD117^+$ and $CD44^-CD117^-$ cells were used to establish the xenograft model and cells were treated with PTX and/or CCL20, followed by proliferation, apoptosis, reactive oxygen species (ROS) and mechanism analyses. Higher expression levels of Oct4, CCR6, Notch1 and ATP binding cassette subfamily G member 1 (ABCG1), increased sphere formation ability, IC_{50} and proliferative ability, as well as lower ROS levels and apoptosis were observed in $CD44^+CD117^+$ cells compared with the $CD44^-CD117^-$ cells. It was found that CCL20 could significantly increase the expression levels of Oct4, CCR6, Notch1 and ABCG1, enhance the IC_{50}, sphere formation ability and proliferation, as well as decrease the ROS and apoptosis levels in the $CD44^+CD117^+$ cells. However, Notch1 knockdown could markedly reverse these changes. Moreover, CCL20 could significantly increase the proliferation and expression levels of Oct4, CCR6, Notch1 and ABCG1 in the $CD44^+CD117^+$ groups compared with the $CD44^-CD117^-$ groups. After treatment with PTX, apoptosis and ROS levels were decreased in the $CD44^+CD117^+$ groups compared with the $CD44^-CD117^-$ groups. Collectively, the present results demonstrated that, via the Notch1 pathway, CCL20/CCR6 may promote the stemness and PTX resistance of $CD44^+CD117^+$ cells in ovarian cancer.

Correspondence to: Professor Yongjie Tian, Department of Obstetrics and Gynecology, Shandong Provincial Hospital, Cheeloo College of Medicine, Shandong University, 324 Jingwuweiqi Road, Jinan, Shandong 250021, P.R. China
E-mail: yongjie_tian@126.com

Dr Li Zhao, Department of Obstetrics and Gynecology, Taian City Central Hospital, 29 Longtan Road, Taian, Shandong 271000, P.R. China
E-mail: fuchan2006@163.com

*Contributed equally

Key words: ovarian cancer stem-like cells, paclitaxel resistance, C-C motif chemokine ligand 20/C-C motif chemokine receptor 6 axis, notch receptor 1 pathway

Introduction

One of the most common lethal malignancies in women worldwide is ovarian cancer (1). Ovarian cancer is ranked as the 7th most prevalent female cancer type, as shown by a 2018 report, accounting for >180,000 deaths in China (2). Moreover, ~70% of ovarian cancer is diagnosed at an advanced stage due to silent symptoms, the hidden growth of the tumor and the lack of appropriate early diagnostic methods (3). Despite advancements in chemotherapy and surgery, the prognosis of patients with ovarian cancer has not changed significantly over the last few decades. Moreover, drug resistance has become a new challenge for the therapy of ovarian cancer (4). Thus, it is important to illustrate the mechanism of drug resistance and overcome this challenge for improving the therapy and prognosis of ovarian cancer.

The standard treatment for ovarian cancer is surgery combined with paclitaxel (PTX)- and platinum-based adjuvant chemotherapy (5). However, the first line obstruction in ovarian cancer treatment is PTX and platinum resistance (6). As indicated by the mechanism of the drug-resistant tumor, there may be a pool of self-renewing malignant cells, namely ovarian cancer stem-like cells, which could enhance the self-renewal, reproduction and drug resistance of tumors, thereby serving key roles in the initiation, diffusion, metastasis

and recurrence of cancer (7,8). As shown in previous studies, a potential marker for ovarian stem-like cancer cells could be CD44, along with CD117 (9,10). Increased expression levels of CD44, CD117 and aldehyde dehydrogenase 1 family member A1 in SKOV3 cells are significantly correlated with the enhancing features of epithelial-mesenchymal transition (EMT), sphere formation, metastasis and multidrug resistance abilities (11,12). At present, the sensitivity of CD44$^+$CD117$^+$ cells to chemotherapy drugs, including PTX, remains unknown and needs to be further investigated. Moreover, in the drug resistance of ovarian cancer, the exact mechanism of cancer stem-like cells are yet to be fully elucidated.

C-C motif chemokine ligand 20 (CCL20), as a ligand of C-C motif chemokine receptor 6 (CCR6), serves a key role in the development of numerous cancer types, such as lung cancer, colorectal cancer and thyroid cancer (13,14). Moreover, the CCL20/CCR6 axis serves an important role in the process of drug resistance (15). As shown in a recent study, cisplatin can stimulate macrophages to secrete CCL20 and promote ovarian cancer cell migration via the CCL20/CCR6 axis (16). However, in ovarian cancer, the role of the CCL20/CCR6 axis and its mechanism remain unclear and require further examination.

In embryonic development and numerous cellular physiological processes, notch receptor (Notch) is involved in regulating cell proliferation, apoptosis and differentiation (17). As a member of the Notch family, Notch1 is implicated in multiple cancer types, such as breast cancer (especially triple-negative breast cancer), leukemias and brain tumors, among others (18,19). Notch1 is closely associated with numerous signaling pathways that are therapeutically involved in tumorigenesis, such as TLR4/NF-κB and PI3K/AKT (20). Together these impact apoptosis, proliferation, chemosensitivity, immune response and the population of cancer stem cells.

In the present study, a population of CD44$^+$CD117$^+$ subgroup cells was isolated from SKOV3 cells, followed by determining their stemness and drug resistance. Furthermore, the underlying mechanism of CD44$^+$CD117$^+$ cells in drug resistance and stemness maintenance was examined. The current study also provides novel insights into the mechanism and clinical therapy of PTX resistance in ovarian cancer.

Materials and methods

Cell culture and isolation. The human ovarian cancer cell line, SKOV-3, was purchased from The Shanghai Stem Cell Institute, and was cultured in DMEM (Invitrogen; Thermo Fisher Scientific, Inc.) supplemented with 10% FBS (Gibco; Thermo Fisher Scientific, Inc.) and 1% penicillin-streptomycin mixture (Sigma-Aldrich; Merck KGaA) at 37˚C in a humidified atmosphere with 5% CO_2.

CD44$^+$CD117$^+$ cells were then separated from SKOV-3 cells using the magnetic-activated cell sorting kit (Miltenyi Biotec GmbH) according to the manufacturer's instructions. The kit included CD44$^+$ and CD117$^+$ antibodies. CD44$^+$ cells were sorted using a mouse anti-human CD44$^+$ antibody combined with magnetic microbeads. After magnetic column depletion, among CD44$^+$ SKOV3 cells, CD117$^+$ cells were isolated using CD117$^+$ antibody combined with magnetic microbeads. Moreover, among CD44$^-$ cells, the CD117$^+$ subset was isolated using CD117$^+$ antibody combined with magnetic microbeads. The CD44$^+$CD117$^+$ stem-like subsets and CD44$^-$CD117$^-$ cells were harvested after magnetic column depletion and maintained in a DMEM/F12 medium containing 5 μg/ml insulin (Sigma-Aldrich; Merck KGaA), 10 ng/ml basic fibroblast growth factor (bFGF; Sigma-Aldrich; Merck KGaA), 20 ng/ml human recombinant epidermal growth factor (EGF; Sigma-Aldrich; Merck KGaA) and 0.5% FBS.

Construction of transient small interfering RNA (siRNA/si) Notch1 cell lines. According to GenBank (NM_017617.4), a siRNA sequence of human Notch1 was designed. The sequence was as follows: siNotch1-1 forward (F), 5'-AGU GGACAUCAGUACUGUA-3' and reverse (R), 3'-UACAGU ACUGAUGUCCACU-5'; siNotch1-2 F, 5'-AUGCGGGCA AGUGCAUCAACA-3' and R, 3'-UGUUGAUGCACUUGC CCGCAU-5'; and siNotch1-3 F, 5'-GCUACACAGGGAGC AUGUGUA-3' and R, 3'-TACACATGCTCCCTGTGTAG C-5'. The negative control (siNC) was designed as follows: F, 5'-UUCUCCGAACGUGUCACGUTT-3' and R, 3'-ACGUGA CACGUUCGGAGAATT-5'. All primers were synthesized and recombined to the plasmids (pcDNA3.1) by Shanghai GenePharma Co., Ltd.. After cells were inoculated overnight in a 6-well plate with 60% confluency, 20 μl siNotch1 or siNC recombinant were transfected into cells using Lipofectamine® 2000 (Invitrogen; Thermo Fisher Scientific, Inc.), according to the manufacturer's protocol at 37˚ and 5% CO_2 in an incubator and for the following experiments 48 h later as indicated.

Xenograft and grouping. In total, 16 male nude mice (age, 6-8 weeks; weight, 25-30 g) were purchased from the Experimental Animal Center of the Shandong University and raised at the Experimental Animal Center. Mice were housed at 25±1˚C with 12-h light/dark cycles, 50±5% humidity and free access to food and water. The mice were randomly divided into four groups: i) CD44$^+$CD117$^+$ + PTX (Beijing Solarbio Science & Technology Co., Ltd.) group (n=4); ii) CD44$^+$CD117$^+$ + PTX + CCL20 (Beijing Solarbio Science & Technology Co., Ltd.) group (n=4); iii) CD44$^-$CD117$^-$ + PTX group (n=4); and iv) CD44$^-$CD117$^-$ + PTX + CCL20 group (n=4). For xenografts, CD44$^+$CD117$^+$ ($2x10^6$) subsets or CD44$^-$CD117$^-$ subsets cells ($2x10^6$) suspended in 0.5 ml PBS were subcutaneously injected into the left flank of each nude mouse to establish tumors. Then, PTX (10 mg/kg) and/or CCL20 (1 mg/kg) were injected intraperitoneally simultaneously on days 1, 3 and 7. Tumor size was monitored on the 3rd, 7th, 14th, 21st and 28th days (15). At the end of the experiment and under continuous anesthesia, the animals were euthanized by an overdose of pentobarbital (125 mg/kg). All experiments were approved by The Animal Care and Use Committee of the Shandong Provincial Hospital, Cheeloo College of Medicine, Shandong University.

Tumor sphere formation assay. In a 24-well plate, CD44$^+$CD117$^+$ or CD44$^-$CD117$^-$ cells were harvested, counted and seeded with a low attachment (Corning, Inc.) at a density of $1.0x10^3$ per well after isolation or treatment. Then, the cells were maintained in a DMEM/F12 medium (Sigma-Aldrich; Merck KGaA), without FBS, supplemented with 4 mg/ml heparin

(Sigma-Aldrich; Merck KGaA), 20 ng/ml EGF (Sigma-Aldrich; Merck KGaA), 20 ng/ml bFGF (Sigma-Aldrich; Merck KGaA) and 2% B27 (Invitrogen; Thermo Fisher Scientific, Inc.). After 10-14 days, spheres were analyzed and images were captured with an inverted fluorescent microscope (Nikon Ni-U; Nikon Corporation; magnification, x100).

Cytotoxicity determination. The IC_{50} of cells exposed to PTX was determined using a Cell Counting Kit (CCK)-8 assay (Dojindo Molecular Technologies, Inc.) according to the manufacturer's instructions. In brief, cells were inoculated at a concentration of $4x10^3$/100 μl per well and cultured at 37˚C for 12 h in a 96-well plate. The cells were then maintained at 37˚C with 200 μl fresh medium containing different concentrations of PTX (0-50 nM) for 48 h. Following this, the cells were incubated with 20 μl CCK-8 solution at 37˚C for 24 h. Then, the optical density value of each well was detected using a microplate reader at 450 nm (Thermo Fisher Scientific, Inc.).

Reactive oxygen species (ROS) detection. For ROS detection, $5x10^5$ cells were seeded overnight in a 6-well plate and then treated with PTX (5 nM) at 37˚C for 48 h. Subsequently, 5 μM carboxy 2'-7'-dichlorofluorescein diacetate was added in Hanks' Balanced Salt Solution and incubated with cells at room temperature for 0.5 h. Fresh tissues were harvested, followed by a single cell suspension preparation. Tissue was digested with trypsin to obtain single cell suspension. Cells were then inoculated in a 6-well plate as aforementioned. The levels of intracellular peroxide were measured using a flow cytometer (BD FACSAria; BD Biosciences) at 485 nm excitation and 520 nm emission to analyze the ROS generation.

Analysis of apoptosis. The apoptosis of cells was determined using flow cytometry and Hoechst assays. SKOV3 cells were seeded in a 6-well plate for flow cytometry and treated with PTX (5 nM) at 37˚C for 48 h. The adherent and floating cells were harvested, washed with cold PBS and stained with FITC-conjugated Annexin V/PI (Beijing Solarbio Science & Technology Co., Ltd.), according to the manufacturer's instructions. The double-stained cells were then detected via Accuri C6 plus flow cytometry (BD Bioscience).

For Hoechst staining, $5x10^5$ cells were seeded overnight in a 6-well plate and treated with PTX (5 nM) at 37˚C for 48 h. Cells were then stained with 0.5 μg/ml Hoechst 33342 dye in a 5% CO_2 incubator at 37˚C for 25 min and were analyzed using a Nikon Ni-U fluorescence microscope (Nikon Corporation; magnification, x100).

H&E staining. The tumors were removed and were fixed with 4% paraformaldehyde at 37˚C for >24 h. Specimens were then dehydrated in isopropyl alcohol by xylene and embedded in paraffin. According to the manufacturer's instructions, specimens were cut into slices (thickness, 5 μm) and stained with H&E (Nanjing Jiancheng Bioengineering Institute) at 37˚C for 24 h. For subsequent analysis, the slices were dehydrated and sealed with neutral resins. Images were captured with an inverted fluorescent microscope (Nikon Ni-U; Nikon Corporation; magnification, x100). A total of 3 field of view were observed by microscopy.

TUNEL assay. The apoptosis of tumor tissue slices was assessed using the Clicl-iT Plus TUNEL assay (Thermo Fisher Scientific, Inc.). The tumors were removed and were fixed with 4% paraformaldehyde at 37˚C for 24 h. According to the manufacturer's instructions, specimens were sectioned at 5 μm and stained with TUNEL reagent (Nanjing Jiancheng Bioengineering Institute) at 37˚C for 1 h. After staining, the sections were sealed with a Prolong Gold antifade reagent with DAPI and images were captured with an inverted fluorescent microscope (Nikon Ni-U; Nikon Corporation; magnification, x100). A total of 3 field of view were observed by microscopy.

Immunohistochemistry (IHC). IHC was used to detect the expression level of CCR6 in xenograft mice. The tumors were removed and were fixed with 4% paraformaldehyde at 37˚C for 48 h. To retrieve the antigen, 5-μm-thick slices from the center of paraffin-embedded tumor samples were collected, deparaffinized in xylene, rehydrated with gradient ethanol, immersed in a 10 mM citrate buffer (pH 6.0) and then heated in a microwave oven for 10 min. Subsequently, slices were incubated with 0.3% H_2O_2 at room temperature for 30 min to block the endogenous peroxidase activity and then with 1.5% normal goat serum at 37˚C for 30 min (Takara Biotechnology Co., Ltd.) for blocking non-specific protein binding. Subsequently, the slices were immersed in the primary antibody in a humidity chamber at 4˚C overnight. Slices were then incubated with a biotinylated goat anti-mouse IgG antibody (1:1,000; cat. no. AP124; Sigma-Aldrich; Merck KGaA) at 37˚C for 30 min and visualized using the 3'3-diaminovbenzidine method. For further analysis, slices were then counterstained with hematoxylin for 30 min at 37˚C and sealed with neutral resins. Images were captured with an inverted fluorescent microscope (Nikon Ni-U; Nikon Corporation; magnification, x100).

Reverse transcription-quantitative (RT-q) PCR. TRIzol® reagent (Takara Biotechnology Co., Ltd.) was used to isolate total RNA samples from cells and tissues according to the manufacturer's instructions. A RT-qPCR kit (Takara Biotechnology Co., Ltd.) was used for cDNA synthesis, according to the manufacturer's instructions. With cDNA as a template, RT-qPCR was performed using SYBR Green (Takara Biotechnology Co., Ltd.) in an ABI 6500 system (Applied Biosciences; Thermo Fisher Scientific, Inc.) under the following conditions: Initial denaturation at 95˚C for 90 sec, followed by 40 cycles of 95˚C for 15 sec, 58˚C for 21 sec and 72˚C for 24 sec. The primers of genes are presented in Table I. With GAPDH as the internal control, the relative gene expression was calculated using the $2^{-\Delta\Delta Cq}$ method (21).

Western blotting. The cells and tissue samples were lysed with a RIPA lysis buffer containing protease inhibitors (Sigma-Aldrich; Merck KGaA). The protein suspension was then collected and quantified using the BCA Protein Assay kit (Pierce; Thermo Fisher Scientific, Inc.). Then, 5 μg protein was boiled with a load buffer for 10 min, separated with 10% SDS-PAGE and transferred onto PVDF membranes (MilliporeSigma). Then, 5% skimmed milk was used to block the membrane at room temperature for 0.5 h, followed by primary antibody incubation at 4˚C overnight. After washing with TBS -0.05% Tween-20 and polysorbate buffer,

Table I. Primers for reverse transcription-quantitative PCR detection.

Gene ID	Sequence (5'-3')	Product length (bp)
OCT4-F	ATCGAGAACCGAGTGAGAGG	120
OCT4-R	CACTCGGACCACATCCTTCT	
CCR6-F	TTCAGCGATGTTTTCGACTCC	134
CCR6-R	GAAATCGGTACAAATAGCCTGG	
GAPDH-F	TGTTCGTCATGGGTGTGAAC	154
GAPDH-R	ATGGCATGGACTGGTCAT	
Notch1-F	GAGGCGTGGCAGACTATGC	140
Notch1-R	CTTGTACTCCGTCAGCGTGA	

F, forward; R, reverse; CCR6, C-C motif chemokine receptor 6.

the membrane was incubated at room temperature with the secondary antibodies for 1 h. The secondary antibodies were horseradish peroxidase-labeled goat anti-rabbit IgG (1:5,000; cat. no. AP156P; Sigma-Aldrich; Merck KGaA) or goat anti-mouse IgG (1:5,000; cat. no. AP-308P; Sigma-Aldrich; Merck KGaA). The protein bands were visualized using an enhanced chemiluminescence kit (Beyotime Institute of Biotechnology) according to the manufacturer's protocol and quantified using the Gel-Pro-Analyzer 4.0 software (Media Cybernetics, Inc.). The primary antibodies were: CCR6 (1:1,000; cat. no. GTX71397; GeneTex, Inc.), ATP binding cassette subfamily G member 1 (ABCG1; cat. no. ab201776; 1:1,000; Abcam), Oct4 (1:1,000; cat. no. ab200834; Abcam), Notch1 (1:1,000; cat. no. 4380; Cell Signaling Technology, Inc.) and GAPDH (1:5,000; cat. no. SAB2103104; Sigma-Aldrich; Merck KGaA).

Statistical analysis. GraphPad Prism 7.0 (GraphPad Software, Inc.) was used for statistical analysis. All experiments were conducted in triplicate, and the data are presented as the mean ± SD. Comparisons between groups were conducted using paired Student's t-test, and multiple comparisons were made using a one-way ANOVA, followed by Tukey's test. $P<0.05$ was considered to indicate a statistically significant difference.

Results

CD44$^+$CD117$^+$ subgroup cells present higher stemness and PTX resistance than CD44$^-$CD117$^-$cells. The results demonstrated that the expression levels of CD44 and CD117 in the total subclones was significantly increased ($P<0.05$; Fig. S1). Once cells were isolated, CCR6 and Oct4 expression was determined using RT-qPCR. It was found that both Oct4 and CCR6 expression levels were significantly increased in CD44$^+$CD117$^+$ cells compared with CD44$^-$CD117$^-$ cells ($P<0.0001$ and $P<0.001$; Fig. 1A). CD44$^+$CD117$^+$ cells also showed a higher sphere formation ability compared with CD44$^-$CD117$^-$ subgroup cells, as detected in the sphere formation assay (Fig. 1B). Moreover, CD44$^+$CD117$^+$ subgroup cells exhibited significant higher protein expression levels of Oct4, CCR6, Notch1 and ABCG1 than CD44$^-$CD117$^-$ cells ($P<0.001$; Fig. 1C and D).

Considering these findings, the PTX resistance of cells was determined using CCK-8 assay. The results indicated that the IC_{50} of CD44$^+$CD117$^+$ subgroup cells for PTX at 24 h (10.22 nM) and 48 h (5.04 nM) was higher compared with that in CD44$^-$CD117$^-$ subgroups at 24 h (4.99 nM) and 48 h (2.51 nM), respectively (Fig. 1E). Moreover, the ROS level was lower in CD44$^+$CD117 cells compared with CD44$^-$CD117$^-$ cells after treatment with PTX (Fig. 2A and B). Furthermore, a lower apoptotic rate was observed in CD44$^+$CD117$^+$ subgroup cells compared with that in CD44$^-$CD117$^-$ subgroup cells after treatment with PTX ($P<0.01$, Fig. 2C and D). The CCK-8 assay also indicated that CD44$^+$CD117$^+$ cells showed increased proliferation compared with CD44$^-$CD117$^-$ cells after treatment with PTX ($P<0.05$ and $P<0.001$; Fig. 2E). These findings suggest that increased stemness and PTX resistance were observed in CD44$^+$CD117$^+$ subgroup cells than in CD44$^-$CD117$^-$ cells, which could be attributed to the involvement of the Notch1 signaling pathway.

Silencing Notch1 reverses the effect of CCL20 on enhancing the stemness and PTX resistance of CD44$^+$CD117$^+$ cells. In order to investigate the underlying pathway involved in the regulation of stemness and PTX resistance, Notch1 was silenced in CD44$^+$CD117$^+$ cells that were treated with CCL20, a ligand of CCR6, followed by stemness and PTX resistance analyses. It was found that transfection of siNotch1 significantly inhibited the mRNA and protein expression levels of Notch1 ($P<0.05$, $P<0.01$ and $P<0.001$; Fig. S1).

The RT-qPCR analysis revealed that CCL20 treatment could significantly increase the expression level of Oct4, but silencing Notch1 could markedly reverse this upregulation in CD44$^+$CD117$^+$ cells ($P<0.001$; Fig. 3A). Moreover, via western blot analysis, it was identified that the protein expression levels of Oct4, ABCG1 and CCR6 in CD44$^+$CD117$^+$ cells were significantly be increased by CCL20, but that siNotch1 could markedly reverse the effect of CCL20 in elevating Oct4, ABCG1 and CCR6 expression in CD44$^+$CD117$^+$ cells ($P<0.001$ and $P<0.001$; Fig. 3B and C). Sphere formation assays also demonstrated that CCL20 could increase the sphere formation capacity of CD44$^+$CD117$^+$ cells, while siNotch1 could notably impair the promotive effect of CCL20 (Fig. 3D). Thus, it was suggested that the CCL20/CCR6 axis may increase the stemness of CD44$^+$CD117$^+$ cells via the Notch1 pathway.

Next, the PTX resistance of CD44$^+$CD117$^+$ cells after transfection with siNotch1 and CCL20 treatment was determined. The results demonstrated that CCL20 could markedly increase IC_{50} of CD44$^+$CD117$^+$ cells (IC_{50}=17.51 nM, 8.41 nM) to PTX compared with the control group (IC_{50}=10.98 nM, 4.86 nM) at 24 and 48 h, while siNotch1 could significantly reverse the effect of CCL20 on PTX resistance of CD44$^+$CD117$^+$ at 24 h (IC_{50}=7.92 nM, 4.22 nM; Fig. 4A), respectively. After further analysis, it was observed that CCL20 could also markedly ameliorate the ROS level in CD44$^+$CD117$^+$ cells induced by PTX, while siNotch1 could attenuate the effect of CCL20 in alleviating ROS levels in CD44$^+$CD117$^+$ cells after treatment with PTX (Fig. 4B). Moreover, the apoptosis of CD44$^+$CD117$^+$ cells was significantly decreased by CCL20 after treatment with PTX ($P<0.0001$), but siNotch1 could partially reverse the

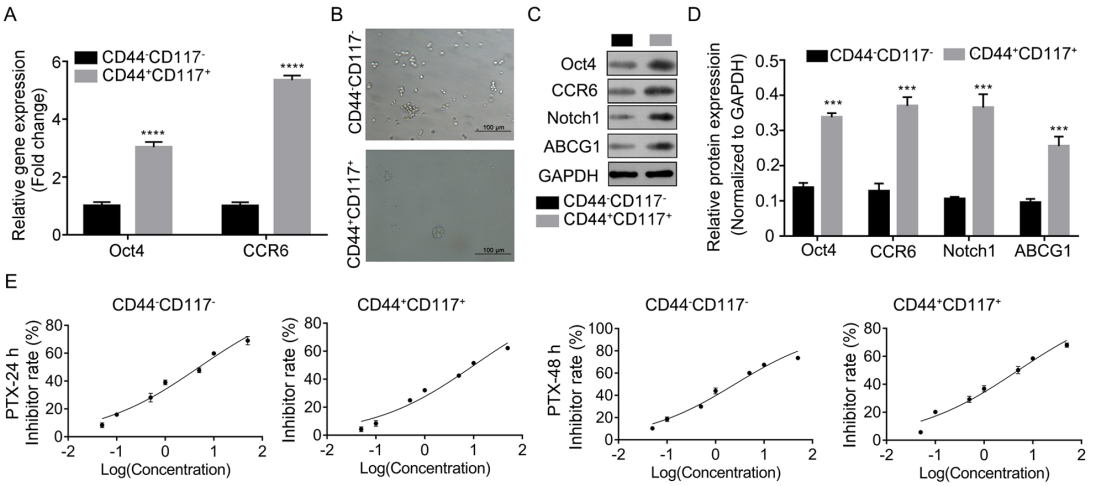

Figure 1. CD44$^+$CD117$^+$ cells have a powerful PTX resistance compared with CD44$^-$CD117$^-$ cells. (A) Expression levels of Oct4 and CCR6 were determined via reverse transcription-quantitative PCR. (B) Sphere formation analysis of CD44$^+$CD117$^+$ and CD44$^-$CD117$^-$ cells. (C) Expression levels of Oct4, CCR6, Notch1 and ABCG1 were determined via western blotting. (D) Semi-quantitative results of protein expression. (E) IC_{50} of CD44$^+$CD117$^+$ and CD44$^-$CD117$^-$ cells to PTX at 24 and 48 h. ***P<0.001 and ****P<0.0001 vs. CD44$^-$CD117$^-$ group. PTX, paclitaxel; CCR6, CCR6, C-C motif chemokine receptor 6; Notch1, notch receptor 1; ABCG1, ATP binding cassette subfamily G member 1.

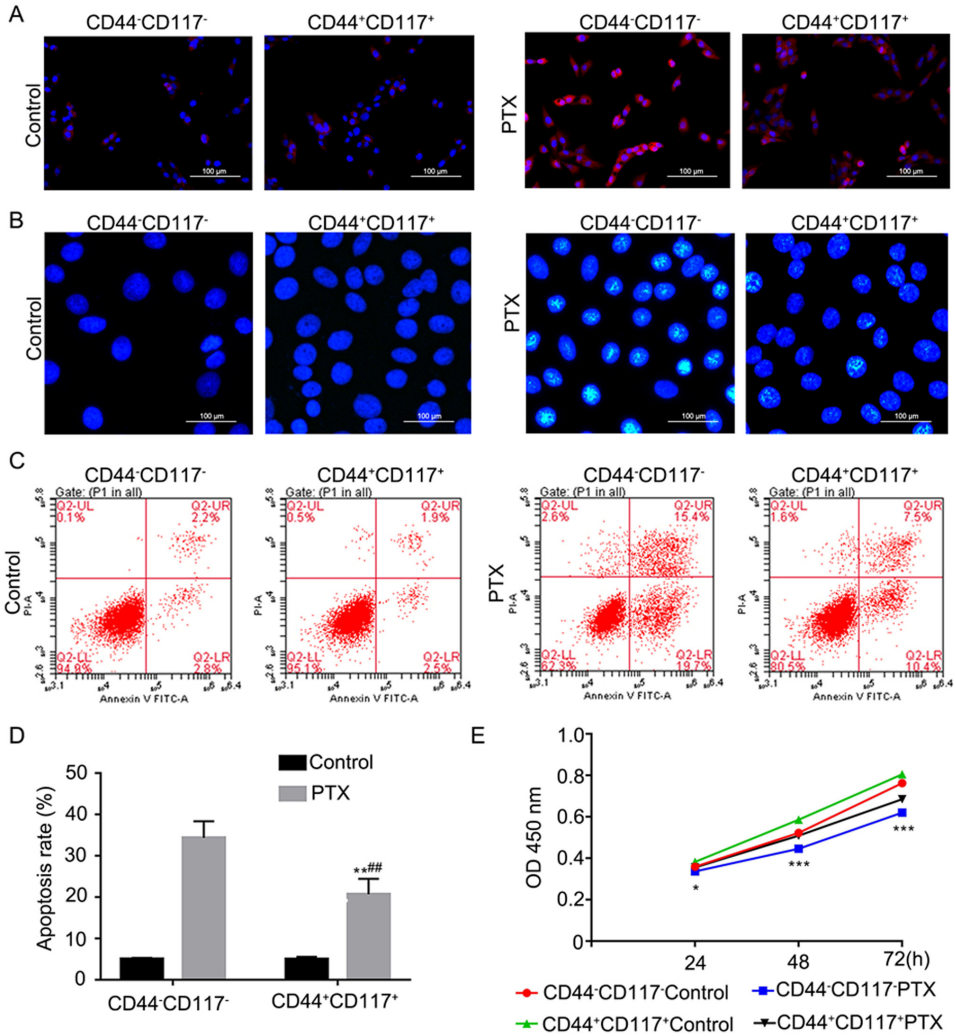

Figure 2. CD44$^+$CD117$^+$ cells show increased stemness compared with CD44$^-$CD117$^-$ cells. (A) Dichlorofluorescin diacetate staining detected the ROS levels of CD44$^+$CD117$^+$ and CD44$^-$CD117$^-$ cells after treatment with PTX for 48 h. (B) Hoechst assay detected the apoptosis of CD44$^+$CD117$^+$ and CD44$^-$CD117$^-$ cells after treatment with PTX for 48 h. Scale bar, 100 μm. (C) Flow cytometry results of the apoptosis of CD44$^+$CD117$^+$ and CD44$^-$CD117$^-$ cells after treatment with PTX for 48 h. (D) Quantitative results of apoptosis. (E) Cell Counting Kit-8 results of the proliferation of CD44$^+$CD117$^+$ and CD44$^-$CD117$^-$ cells after treatment with PTX for 48 h. *P<0.05, **P<0.01 and ***P<0.001 vs. CD44$^-$CD117$^-$ + PTX group; $^{\#\#}$P<0.01 vs. CD44$^+$CD117$^+$ control group. PTX, paclitaxel; OD, optical density.

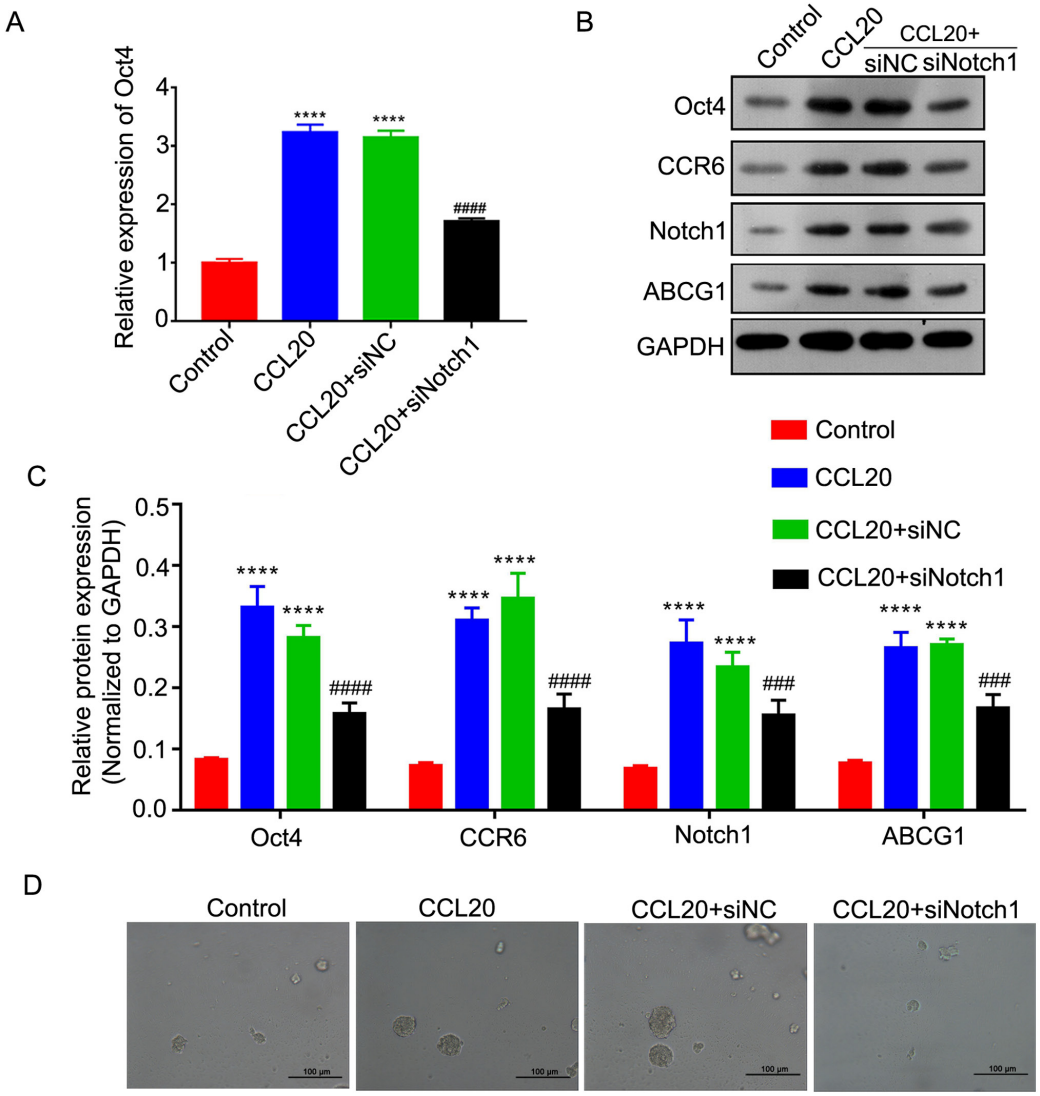

Figure 3. siNotch1 reverses the effect of the CCL20/CCR6 axis in enhancing the stemness of CD44+CD117+ cells. (A) Expression level of Oct4, as determined by reverse transcription-quantitative PCR. (B) Protein expression levels of Oct4, CCR6, Notch1 and ABCG1 were determined via western blotting. (C) Semi-quantitative analysis of Oct4, CCR6, Notch1 and ABCG1 protein expression. (D) Sphere formation analysis of CD44+CD117+ cells. Scale bar, 100 μm. ****P<0.0001 vs. Control group; ###P<0.001 and ####P<0.0001 vs. CCL20 group. NC, negative control; si, small interfering RNA; CCR6, CCR6, C-C motif chemokine receptor 6; CCL20, C-C motif chemokine ligand 20; ABCG1, ATP binding cassette subfamily G member 1; Notch1, notch receptor 1.

effect of CCL20 in suppressing apoptosis of CD44+CD117+ cells induced by PTX (P<0.001; Fig. 4C-E). In addition, the CCK-8 assays identified that CCL20 could increase the proliferation of CD44+CD117+ cells, and the promotive effect of CCL20 after treatment with PTX could be impaired by siNotch1 (Fig. 4F). This evidence suggested that the CCL20/CCR6 axis nay increase the stemness and PTX resistance of CD44+CD117+ cells via the Notch1 signaling pathway.

A CCL20/CCR6 axis promotes tumorigenicity and PTX resistance of CD44+CD117+ cells in ovarian cancer via the Notch1 signaling pathway. To confirm the role of the CCL20/CCR6 axis in PTX resistance, SKOV3 CD44+CD117+ and CD44-CD117- subgroup cells were subjected to the xenograft assay, followed by CCL20 and/or PTX treatment. The results demonstrated that CCL20 could significantly increase the tumor volume of CD44+CD117+ and CD44-CD117- cells in nude mice compared with the respective PTX treatment alone groups (Fig. 5A and B). From the tumor growth curve analysis, it was found that tumors formed by CD44+CD117+ cells grew more quickly than those formed by CD44-CD117- (P<0.001; Fig. 5B). The growth of all tumors could be significantly increased by treating with PTX, but the volume of tumor-derived from CD44+CD117+ cells was significantly higher compared with that from CD44-CD117- cells (P<0.01; Fig. 5B). Moreover, the weight of tumors derived from CD44+CD117+ cells was significantly greater than that derived from CD44-CD117- cells treated with PTX (P<0.0001; Fig. 5C). The tumor weight was significantly increased by CCL20 treatment in CD44+CD117+ and CD44-CD117- cells treated with PTX. However, tumor weight in the CD44+CD117+ group was significantly higher than that in the CD44-CD117- group (P<0.001; Fig. 5C).

H&E staining analysis tumors of the CD44+CD117+ groups revealed poorly differentiated morphology compared with the CD44-CD117- groups, as characterized by the number of small,

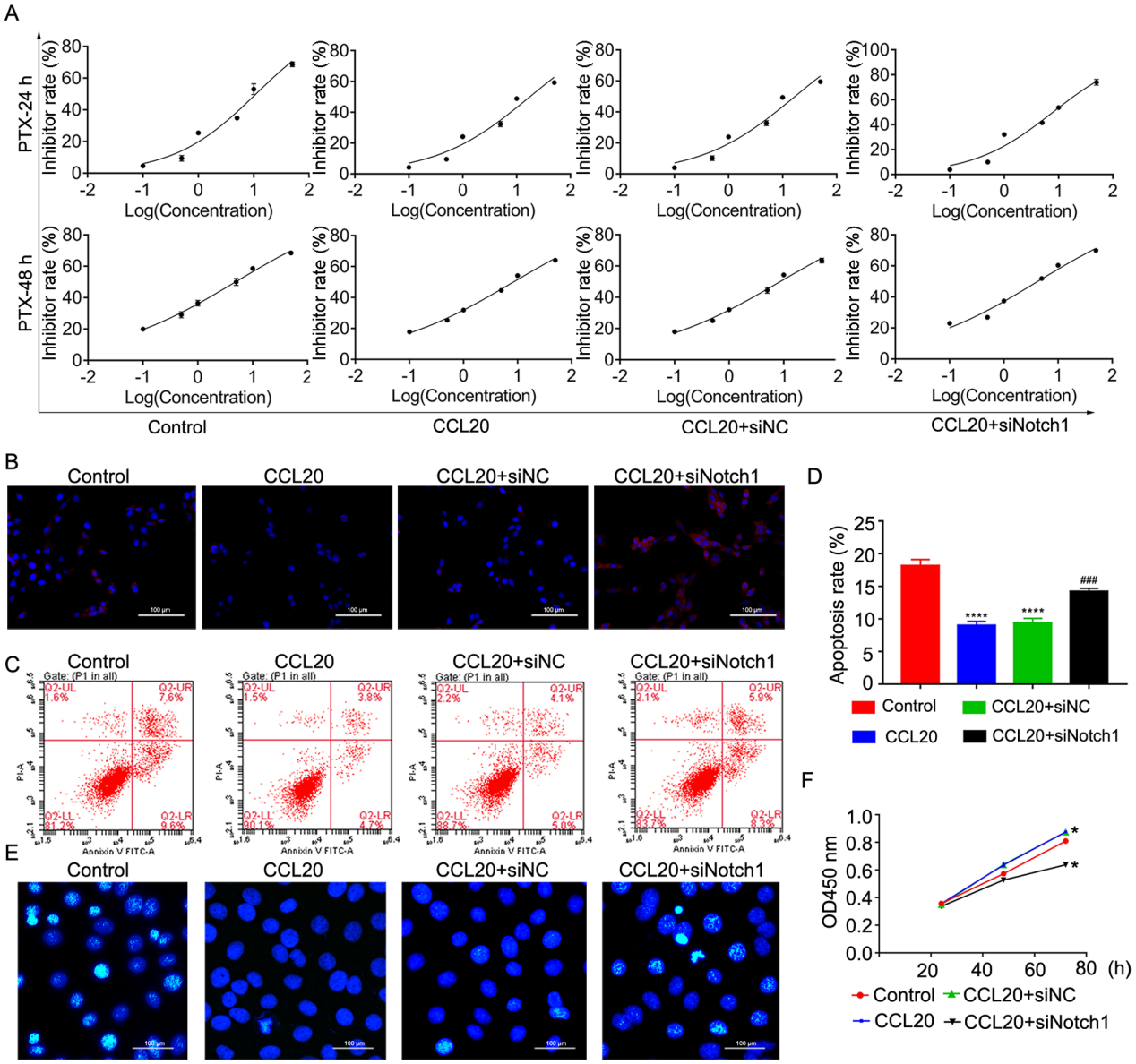

Figure 4. siNotch1 reverses the effect of the CCL20/CCR6 axis in enhancing the drug resistance of $CD44^+CD117^+$ cells. (A) IC_{50} of $CD44^+CD117^+$ cells with different treatments of PTX at 24 and 48 h. (B) Reactive oxygen species levels of $CD44^+CD117^+$ cells were detected using the dichlorofluorescein diacetate method. Scale bar, 100 μm. (C) Apoptosis of $CD44^+CD117^+$ cells, as determined via flow cytometry. (D) Quantitative analysis of apoptosis, as determined by flow cytometry. (E) Apoptosis of $CD44^+CD117^+$ cells was detected using a Hoechst assay. Scale bar, 100 μm. (F) Proliferation of $CD44^+CD117^+$ cells was determined using a Cell Counting Kit-8 assay. *P<0.05 vs. the control and CCL20+siNC groups; ****P<0.0001 vs. control group; $^{###}$P<0.001 vs. CCL20 group. PTX, paclitaxel; OD, optical density; NC, negative control; si, small interfering RNA; CCL20, C-C motif chemokine ligand 20; Notch1, notch receptor 1.

round cells with hyperchromatic nuclei and scanty cytoplasm, after treatment with PTX. CCL20 treatment could notably decrease tumor differentiation in the $CD44^+CD117^+$ group compared with in the $CD44^-CD117^-$ group (Fig. 5D). A higher expression level of CCR6 in the tumors was identified in the $CD44^+CD117^+$ group compared with the $CD44^-CD117^-$ group via the IHC analysis. Furthermore, CCL20 treatment could markedly increase the expression level of CCR6 in tumors of the $CD44^+CD117^+$ group compared with in the $CD44^-CD117^-$ group (Fig. 5E).

As observed in further investigations, the $CD44^+CD117^+$ group tissue presented with higher proliferation but lower apoptosis compared with the tumor tissue of the $CD44^-CD117^-$ group after treatment with PTX (Fig. 6A and B). In the $CD44^+CD117^+$ and $CD44^-CD117^-$ groups, CCL20 treatment could significantly accelerate proliferation but inhibit apoptosis after treatment with PTX. However, these changes in the $CD44^+CD117^+$ group were higher compared with those in the $CD44^-CD117^-$ group (Fig. 6A and B). Furthermore, ROS levels of tumors in the $CD44^+CD117^+$ group were markedly lower compared with those in the $CD44^-CD117^-$ group after treatment with PTX or CCL20 (Fig. 6C). The stemness and involved signaling pathway were also determined in tumor tissue to further confirm the underlying mechanism. The results indicated that the expression levels of Oct4, CCR6, ABCG1 and Notch1 in tumor of $CD44^+CD117^+$ and $CD44^-CD117^-$ groups could be significantly accelerated by CCL20 treatment, while such facilitation was increased in the $CD44^+CD117^+$ group compared with the $CD44^-CD117^-$ group (P<0.0001; Fig. 6D and E). Taken together, these

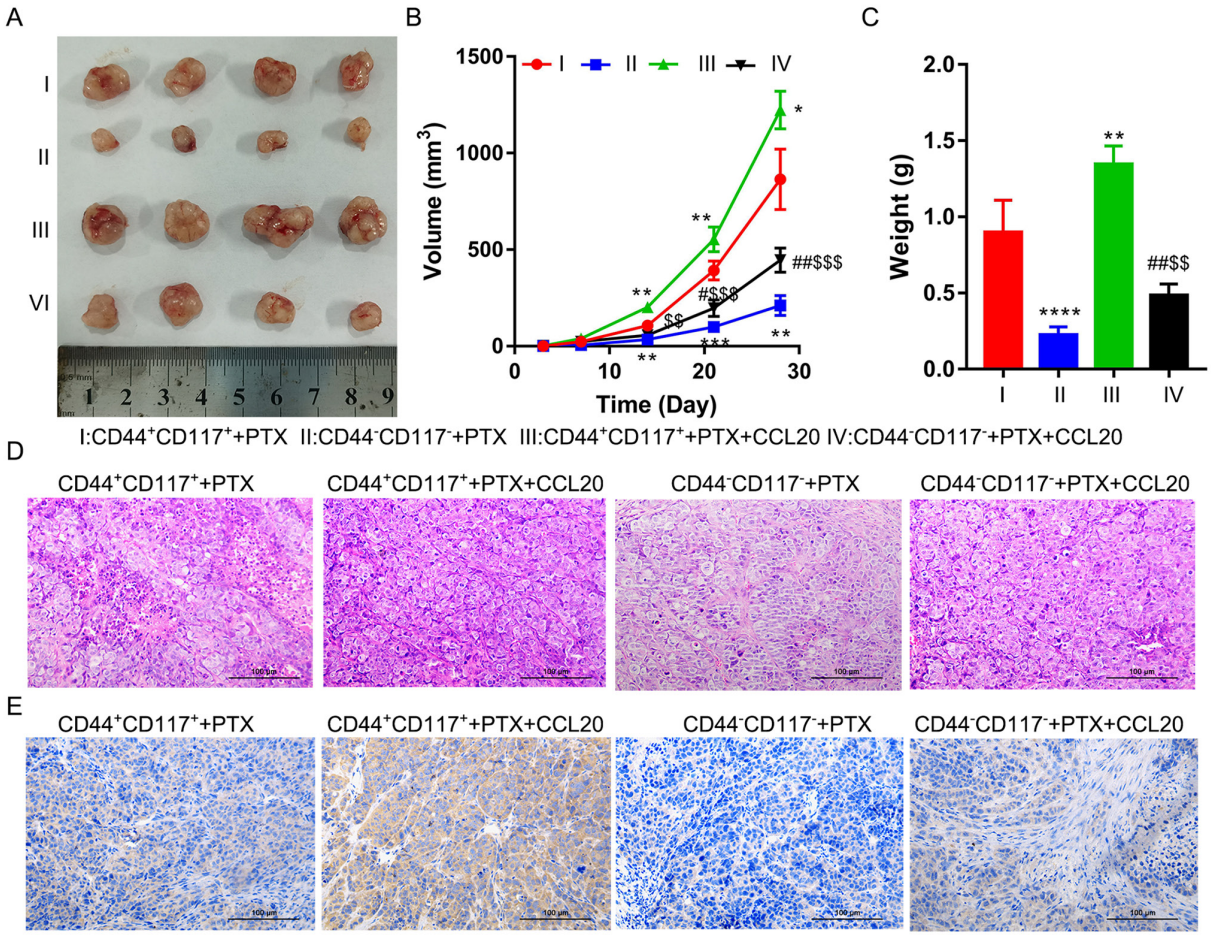

Figure 5. CCL20/CCR6 enhances the stemness and tumorigenicity of CD44⁺CD117⁺ cells treated with PTX via the Notch1 signaling pathway. (A) Image of xenograft tumors derived from CD44⁺CD117⁺ and CD44⁻CD117⁻ cells after a 28-day cultivation. (B) Tumor growth curve of xenograft tumors during the 28-day cultivation. (C) Weight of xenograft tumors after the 28-day cultivation. (D) H&E analysis of tumor lesions. (E) Expression level of CCR6 in tumor was determined via immunohistochemistry. Scale bar, 100 μm. *P<0.05, **P<0.01, ***P<0.001 and ****P<0.0001 vs. CD44⁺CD117⁺ + PTX group; $^{\#}$P<0.05 and $^{\#\#}$P<0.01 vs. CD44⁻CD117⁻ + PTX group; $^{\$\$}$P<0.01 and $^{\$\$\$}$P<0.001 vs. CD44⁺CD117⁺ + PTX ⁺ CCL20 group. PTX, paclitaxel; CCL20, C-C motif chemokine ligand 20.

findings suggested that CCL20/CCR6/Notch1 signaling could markedly facilitate the stemness and proliferation of the CD44⁺CD117⁺ subgroup cancer cells to promote ovarian cancer resistance to PTX.

Discussion

Cancer stem-like cells are widely accepted to be responsible for drug resistance of ovarian cancer (21). Therefore, it is of great significance to reveal the role of cancer stem-like cells in drug resistance. It has been shown that two surface markers of cancer cells in ovarian cancer are CD44 and CD117 (22). In the present study, CD44⁺CD117⁺ subgroup cells were isolated from SKOV3 cells and used for PTX resistance investigation.

Several studies have reported that CD44 and CD117 are two stem cell markers in ovarian cancer, and that CD44⁺CD117⁺ cancer cells present with a powerful survival ability and tumorigenic capability (23,24). In ovarian cancer cells, the overexpression of miR-199a could significantly inhibit CD44 expression and attenuate multidrug resistance and tumorigenicity (25). Moreover, a clinical meta-analysis revealed that a marker for the poor prognosis of ovarian cancer could be the upregulation of CD117 (26). In the present study, CD44⁺CD117⁺ cells were isolated from SKOV3 cells. IC_{50} analysis identified that CD44⁺CD117⁺ cells had a higher IC_{50} concentration of PTX compared with CD44⁻CD117⁻ cells, suggesting that CD44⁺CD117⁺ cells showed a higher PTX resistance. In addition, the expression levels of other cancer stem-like cell markers, including Oct4 and ABCG1, were higher compared with those in the CD44⁻CD117⁻ cells, indicating that CD44⁺CD117⁺ cells had a more powerful stemness ability than CD44⁻CD117⁻ cells. After treatment with PTX in both *in vitro* and *in vivo*, CD44⁺CD117⁺ cells also presented higher sphere formation proliferation abilities, and lower apoptosis and ROS levels. It is well known that oxidative stress is directly assessed by measuring ROS. Moreover, ROS are involved in the regulation of cell inventory and death (27). ROS is also reported to be closely associated with inflammation, aging and chronic diseases, including cancer (28). Collectively, the present results suggested that CD44⁺CD117⁺ cells presented a powerful stemness and tumorigenic capability than CD44⁻CD117⁻ cells.

The only known chemokine ligand for CCR6 is CCL20, and this axis has been reported to serve a critical role in the development of numerous types of cancer, such as lung (29), colorectal (30) and thyroid cancers (31). In a recent study,

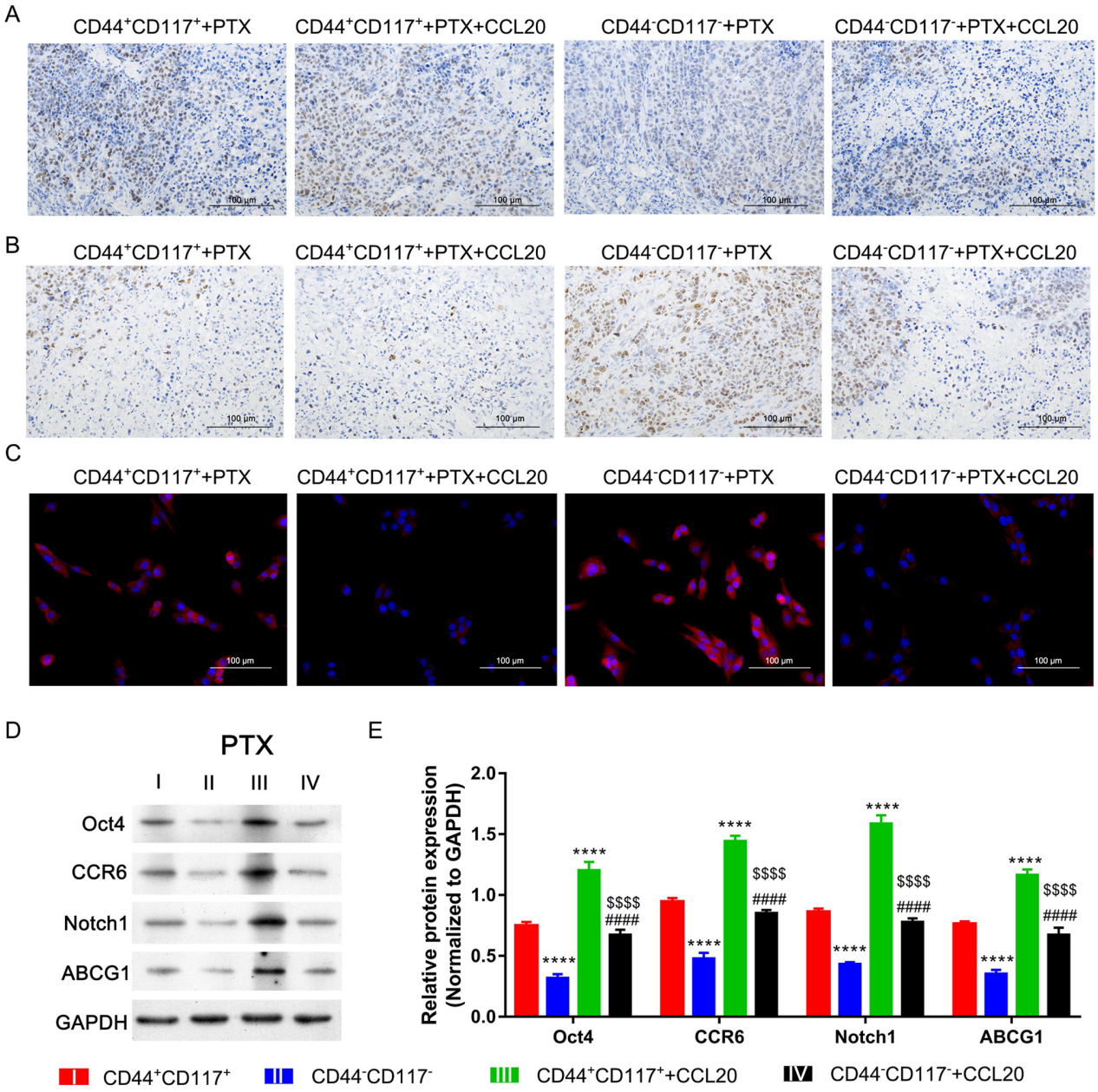

Figure 6. CCL20/CCR6 enhances the stemness and tumorigenicity of $CD44^+CD117^+$ cells treated with PTX via the Notch1 signaling pathway. (A) Expression level of Ki-67 in tumor was determined via immunohistochemistry. (B) Apoptosis of tumor cells was determined using a TUNEL assay. (C) Reactive oxygen species levels of tumors were determined by the dichlorofluorescein diacetate method. Scale bar, 100 μm. (D) Expression levels of Oct4, CCR6, Notch1 and ABCG1 in tumor tissue, as determined via western blotting. (E) Semi-quantitative analysis of Oct4, CCR6, Notch1 and ABCG1 protein expression. ****P<0.0001 vs. $CD44^+CD117^+$ group; $^{\#\#\#\#}$P<0.0001 vs. $CD44^-CD117^-$ group; $^{\$\$\$\$}$P<0.0001 vs. $CD44^+CD117^+$ + CCL20 group. PTX, paclitaxel; CCL20, C-C motif chemokine ligand 20; CCR6, CCR6, C-C motif chemokine receptor 6; Notch1, notch receptor 1; ABCG1, ATP binding cassette subfamily G member 1.

cisplatin was shown to stimulate macrophages to secrete CCL20 and promote ovarian cancer cell migration via the CCL20/CCR6 axis (16). CCL20 can also enhance the chemotherapy resistance of ovarian cancer by regulating ABCB1 expression (31). In the present study, the expression levels of CCL20 and CCR6 were significantly upregulated in $CD44^+CD117^+$ cells compared with those in $CD44^-CD117^-$ cells. Moreover, CCL20 treatment could significantly increase the PTX resistance, proliferation and tumorigenic abilities of $CD44^+CD117^+$ cells, but decreased apoptosis and ROS *in vitro* and *in vivo*.

Accumulating evidence has shown that the CCL20/CCR6 axis also served a critical role in regulating cancer stem cells (15,32-34). However, there are relatively limited associated reports on ovarian cancer. In the current study, it was found that CCL20 treatment could significantly increase the expression levels of stem cell markers, including Oct4, and ABCG1. Previous studies have also suggested that the CCL20/CCR6 axis may play a key role in regulating ovarian cancer stem cells (16,35). Collectively, these findings suggested that the CCL20/CCR6 axis may act as a promotor in maintaining stemness and drug resistance of ovarian cancer. As a ligand of CCR6, CCL20 promotes ovarian stem cells and PTX resistance of ovarian stem cell-like cancer cells. However, whether PTX resistance cancels the silencing of CCR6 needs to be further examined.

A common dysregulated pathway in the development of cancer is the Notch1 signaling pathway, which has been shown to play a critical role in regulating stemness, proliferation, metastasis and drug resistance of cancer (36-38). As shown in a previous study, the hypoxia-induced Notch/SOX2 axis was crucial for maintaining cancer stem-like cells in ovarian cancer (39). It has also been reported that galectin-3 could activate the intracellular domain of Notch1 to maintain the stemness of ovarian cancer stem cells (40). In the present study, it was identified that siNotch1 could significantly decrease the expression levels of Oct4, ABCG1 and CCR6 in CD44$^+$CD117$^+$ cells treated with PTX. Furthermore, the effects of CCL20 could be significantly reversed by siNotch1 to enhance drug resistance and tumorigenic capability, as well as reduce the apoptosis and ROS levels of CD44$^+$CD117$^+$ cells treated with PTX *in vivo* and *in vitro*. Such findings also suggested that the CCL20/CCR6 axis may promote the stemness and tumorigenicity of CD44$^+$CD117$^+$ cells by activating the Notch1 signaling pathway. However, the lack of research on the sensitivity of CD44$^+$CD117$^+$ cells to platinum may be considered a potential limitation of this study.

In conclusion, the present study demonstrated that the CD44$^+$CD117$^+$ subgroup SKOV3 cells showed increased stemness and drug resistance compared with CD44$^-$CD117$^-$ cells. The results indicated that the stemness, tumorigenicity and PTX resistance of CD44$^+$CD117$^+$ cells could significantly enhance CCL20 by activating the Notch1 signaling pathway.

Acknowledgements

Not applicable.

Funding

This study was supported by the Natural Science Foundation of Shandong Province (grant no. 2015GSF118140).

Availability of data and material

The datasets used and/or analyzed during the current study are available from the corresponding author on reasonable request.

Authors' contribution

MC, YT and LZ conceived and designed the research. MC, JS, CF and YL performed the experiments. MC, YT and LZ confirm the authenticity of all the raw data. JS, CF and YL analyzed the data and prepared the figures. MC and JS edited and revised the manuscript. All authors approved the final version of the manuscript.

Ethics approval and consent to participate

The Animal Care and Use Committee of the Shandong Provincial Hospital, Cheeloo College of Medicine, Shandong University, authorized the present study. All methods were carried out in accordance with relevant guidelines and regulations. The animal study was carried out in compliance with the ARRIVE guidelines.

Patient consent for publication

Not applicable.

Competing interests

The authors declare that they have no competing interests.

References

1. Vafadar A, Shabaninejad Z, Movahedpour A, Fallahi F, Taghavipour M, Ghasemi Y, Akbari M, Shafiee A, Hajighadimi S, Moradizarmehri S, *et al*: Quercetin and cancer: New insights into its therapeutic effects on ovarian cancer cells. Cell Biosci 10: 32, 2020.
2. Bray F, Ferlay J, Soerjomataram I, Siegel RL, Torre LA and Jemal A: Global cancer statistics 2018: GLOBOCAN estimates of incidence and mortality worldwide for 36 cancers in 185 countries. CA Cancer J Clin 68: 394-424, 2018.
3. Momenimovahed Z, Tiznobaik A, Taheri S and Salehiniya H: Ovarian cancer in the world: Epidemiology and risk factors. Int J Womens Health 11: 287-299, 2019.
4. Stewart C, Ralyea C and Lockwood S: Ovarian cancer: An integrated review. Semin Oncol Nurs 35: 151-156, 2019.
5. Norouzi-Barough L, Sarookhani MR, Sharifi M, Moghbelinejad S, Jangjoo S and Salehi R: Molecular mechanisms of drug resistance in ovarian cancer. J Cell Physiol 233: 4546-4562, 2018.
6. Damia G and Broggini M: Platinum resistance in ovarian cancer: Role of DNA repair. Cancers (Basel) 11: 119, 2019.
7. Pagotto A, Pilotto G, Mazzoldi EL, Nicoletto MO, Frezzini S, Pastò A and Amadori A: Autophagy inhibition reduces chemoresistance and tumorigenic potential of human ovarian cancer stem cells. Cell Death Dis 8: e2943, 2017.
8. Pieterse Z, Amaya-Padilla MA, Singomat T, Binju M, Madjid BD, Yu Y and Kaur P: Ovarian cancer stem cells and their role in drug resistance. Int J Biochem Cell Biol 106: 117-126, 2019.
9. Klemba A, Purzycka-Olewiecka JK, Wcisło G, Czarnecka AM, Lewicki S, Lesyng B, Szczylik C and Kieda C: Surface markers of cancer stem-like cells of ovarian cancer and their clinical relevance. Contemp Oncol (Pozn) 22: 48-55, 2018.
10. Chung H, Kim YH, Kwon M, Shin SJ, Kwon SH, Cha SD and Cho CH: The effect of salinomycin on ovarian cancer stem-like cells. Obstet Gynecol Sci 59: 261-268, 2016.
11. Zhang S, Balch C, Chan MW, Lai HC, Matei D, Schilder JM, Yan PS, Huang TH and Nephew KP: Identification and characterization of ovarian cancer-initiating cells from primary human tumors. Cancer Res 68: 4311-4320, 2008.
12. Wintzell M, Löfstedt L, Johansson J, Pedersen AB, Fuxe J and Shoshan M: Repeated cisplatin treatment can lead to a multiresistant tumor cell population with stem cell features and sensitivity to 3-bromopyruvate. Cancer Biol Ther 13: 1454-1462, 2012.
13. Chen W, Qin Y and Liu S: CCL20 signaling in the tumor microenvironment. Adv Exp Med Biol 1231: 53-65, 2020.
14. Su S, Sun X, Zhang Q, Zhang Z and Chen J: CCL20 promotes ovarian cancer chemotherapy resistance by regulating ABCB1 expression. Cell Struct Funct 44: 21-28, 2019.
15. Kadomoto S, Izumi K and Mizokami A: The CCL20-CCR6 axis in cancer progression. Int J Mol Sci 21: 5186, 2020.
16. Liu W, Wang W, Wang X, Xu C, Zhang N and Di W: Cisplatin-stimulated macrophages promote ovarian cancer migration via the CCL20-CCR6 axis. Cancer Lett 472: 59-69, 2020.
17. Yi L, Zhou X, Li T, Liu P, Hai L, Tong L, Ma H, Tao Z, Xie Y, Zhang C, *et al*: Notch1 signaling pathway promotes invasion, self-renewal and growth of glioma initiating cells via modulating chemokine system CXCL12/CXCR4. J Exp Clin Cancer Res 38: 339, 2019.
18. Gharaibeh L, Elmadany N, Alwosaibai K and Alshaer W: Notch1 in cancer therapy: Possible clinical implications and challenges. Mol Pharmacol 98: 559-576, 2020.
19. Sanchez-Martin M and Ferrando A: The NOTCH1-MYC highway toward T-cell acute lymphoblastic leukemia. Blood 129: 1124-1133, 2017.
20. Luo Y, Kishi S, Sasaki T, Ohmori H, Fujiwara-Tani R, Mori S, Goto K, Nishiguchi Y, Mori T, Kawahara I, *et al*: Targeting claudin-4 enhances chemosensitivity in breast cancer. Cancer Sci 111: 1840-1850, 2020.

21. Livak KJ and Schmittgen TD: Analysis of relative gene expression data using real-time quantitative PCR and the 2(-Delta Delta C(T)) method. Methods 25: 402-408, 2001.
22. Ning Y, Feng W, Cao X, Ren K, Quan M, Chen A, Xu C, Qiu Y, Cao J, Li X and Luo X: Genistein inhibits stemness of SKOV3 cells induced by macrophages co-cultured with ovarian cancer stem-like cells through IL-8/STAT3 axis. J Exp Clin Cancer Res 38: 19, 2019.
23. Martincuks A, Li PC, Zhao Q, Zhang C, Li YJ, Yu H and Rodriguez-Rodriguez L: CD44 in ovarian cancer progression and therapy resistance-A critical role for STAT3. Front Oncol 10: 589601, 2020.
24. Chen J, Wang J, Chen D, Yang J, Yang C, Zhang Y, Zhang H and Dou J: Evaluation of characteristics of $CD44^{+}CD117^{+}$ ovarian cancer stem cells in three dimensional basement membrane extract scaffold versus two dimensional monocultures. BMC Cell Biol 14: 7, 2013.
25. Zhang R, Zhang P, Wang H, Hou D, Li W, Xiao G and Li C: Inhibitory effects of metformin at low concentration on epithelial-mesenchymal transition of CD44(+)CD117(+) ovarian cancer stem cells. Stem Cell Res Ther 6: 262, 2015.
26. Cheng W, Liu T, Wan X, Gao Y and Wang H: MicroRNA-199a targets CD44 to suppress the tumorigenicity and multidrug resistance of ovarian cancer-initiating cells. FEBS J 279: 2047-2059, 2012.
27. Yang B, Yan X, Liu L, Jiang C and Hou S: Overexpression of the cancer stem cell marker CD117 predicts poor prognosis in epithelial ovarian cancer patients: Evidence from meta-analysis. Onco Targets Ther 10: 2951-2961, 2017.
28. Kleih M, Böpple K, Dong M, Gaißler A, Heine S, Olayioye MA, Aulitzky WE and Essmann F: Direct impact of cisplatin on mitochondria induces ROS production that dictates cell fate of ovarian cancer cells. Cell Death Dis 10: 851, 2019.
29. Moloney JN and Cotter TG: ROS signalling in the biology of cancer. Semin Cell Dev Biol 80: 50-64, 2018.
30. Zhang XP, Hu ZJ, Meng AH, Duan GC, Zhao QT and Yang J: Role of CCL20/CCR6 and the ERK signaling pathway in lung adenocarcinoma. Oncol Lett 14: 8183-8189, 2017.
31. Frick VO, Rubie C, Keilholz U and Ghadjar P: Chemokine/chemokine receptor pair CCL20/CCR6 in human colorectal malignancy: An overview. World J Gastroenterol 22: 833-841, 2016.
32. Zeng W, Chang H, Ma M and Li Y: CCL20/CCR6 promotes the invasion and migration of thyroid cancer cells via NF-kappa B signaling-induced MMP-3 production. Exp Mol Pathol 97: 184-190, 2014.
33. Thapa S and Bhusal K: SUN-545 A rare case of resistance to thyroid hormone due to novel mutation in THRB gene mistreated as hyperthyroidism. J Endocr Soc 3 (Suppl 1): SUN-545, 2019.
34. Ranasinghe R and Eri R: Modulation of the CCR6-CCL20 axis: A potential therapeutic target in inflammation and cancer. Medicina (Kaunas) 54: 88, 2018.
35. Liu W, Wang W, Zhang N and Di W: The role of CCL20-CCR6 axis in ovarian cancer metastasis. Onco Targets Ther 13: 12739-12750, 2020.
36. Zhang J, Yu K, Han X, Zhen L, Liu M, Zhang X, Ren Y and Shi J: Paeoniflorin influences breast cancer cell proliferation and invasion via inhibition of the Notch-1 signaling pathway. Mol Med Rep 17: 1321-1325, 2018.
37. Zhang Z, Han H, Rong Y, Zhu K, Zhu Z, Tang Z, Xiong C and Tao J: Hypoxia potentiates gemcitabine-induced stemness in pancreatic cancer cells through AKT/Notch1 signaling. J Exp Clin Cancer Res 37: 291, 2018.
38. Wang X, Wang R, Bai S, Xiong S, Li Y, Liu M, Zhao Z, Wang Y, Zhao Y, Chen W, *et al*: Musashi2 contributes to the maintenance of CD44v6+ liver cancer stem cells via notch1 signaling pathway. J Exp Clin Canc Res 38: 505, 2019.
39. Seo EJ, Kim DK, Jang IH, Choi EJ, Shin SH, Lee SI, Kwon SM, Kim KH, Suh DS and Kim JH: Hypoxia-NOTCH1-SOX2 signaling is important for maintaining cancer stem cells in ovarian cancer. Oncotarget 7: 55624-55638, 2016.
40. Kang HG, Kim DH, Kim SJ, Cho Y, Jung J, Jang W and Chun KH: Galectin-3 supports stemness in ovarian cancer stem cells by activation of the Notch1 intracellular domain. Oncotarget 7: 68229, 2016.